The Company of
Biologists

RESEARCH ARTICLE

Crosstalk of PD-1 signaling with the SIRT1/FOXO-1 axis during the progression of visceral leishmaniasis

Shalini Roy[1], Shriya Saha[2], Purnima Gupta[2], Anindita Ukil[2] and Pijush K. Das[1],*

ABSTRACT

Previously, we documented the role of the programmed death-1 (PD-1, also known as PDCD1) pathway in macrophage apoptosis and the downregulation of this signaling during infection by the intra-macrophage parasite *Leishmania donovani*. However, we also found that, during the late phase of infection, PD-1 expression was significantly increased without activating host cell apoptosis; here we show that inhibition of PD-1 led to markedly decreased parasite survival, along with increased production of TNFα, IL-12, reactive oxygen species (ROS) and nitric oxide (NO). Increased PD-1 led to inactivation of AKT proteins resulting in nuclear sequestration of FOXO-1. Transfecting infected cells with constitutively active FOXO-1 (CA-FOXO) led to increased cell death, thereby suggesting that nuclear FOXO-1 might be inactivated. Infection significantly induced the expression of SIRT1, which inactivated FOXO-1 through deacetylation, and its knockdown led to increased apoptosis. SIRT1 knockdown also significantly decreased parasite survival along with increased production of TNFα, ROS and NO. Administration of the SIRT1 inhibitor sirtinol (10 mg/kg body weight) in infected mice decreased spleen parasite burden and a synergistic effect was found with PD-1 inhibitor. Collectively, our study shows that *Leishmania* utilizes the SIRT1/FOXO-1 axis for differentially regulating PD-1 signaling and, although they are interconnected, both pathways independently contribute to intracellular parasite survival.

This article has an associated First Person interview with the first author of the paper.

KEY WORDS: *Leishmania donovani*, PD-1, SIRT1, FOXO-1, Apoptosis

INTRODUCTION

Evasion of host cell apoptosis for successful survival is a well-established paradigm of *Leishmania donovani* infection (Akarid et al., 2004; Srivastav et al., 2014). Programmed death 1 receptor (PD-1 also known as PDCD1), a type I transmembrane protein, was initially identified in T cells contributing to T cell apoptosis (Ishida et al., 1992). It is also widely expressed on various immune cells including B cells, NKT cells and macrophages, and interaction with its ligand PD-1L (also known as B7H1, PD-1L1 and CD274) delivers inhibitory signals, that play a pivotal role in impeding T cell functions (Keir et al., 2008). We previously documented that during

[1]Infectious Diseases and Immunology Division, CSIR-Indian Institute of Chemical Biology, Kolkata 700032, India. [2]Department of Biochemistry, Calcutta University, Kolkata 700019, India.

*Author for correspondence (pijushdas@iicb.res.in)

S.R., 0000-0001-8053-1650; S.S., 0000-0002-0710-3913; P.G., 0000-0002-1586-0594; A.U., 0000-0002-2114-6469; P.K.D., 0000-0001-9452-7441

the early phases of infection (0–6 h), *L. donovani*-induced downregulation of PD-1 receptor plays a pivotal role in preventing macrophage-apoptosis (Roy et al., 2017). Interestingly, during late phases of *Leishmania* infection (48–72 h), PD-1 receptor expression was found to be upregulated and, in the present study, we aimed to address the implications of this upregulation.

Downregulation of PD-1 activates pro-survival AKT family proteins (hereafter referred to as AKT), thereby enabling the parasites to escape apoptosis (Roy et al., 2017). Reports have already demonstrated that activation of AKT pathway prevents host cell death during *L. donovani* infection (Ruhland et al., 2007). AKT phosphorylates the pro-apoptotic protein FOXO-1, a member of the Forkhead family of transcription factors. Phosphorylation leads to cytosolic translocation and subsequent degradation of FOXO-1 (Brunet et al., 1999). Infection-induced PD-1 activation during late phases would be expected to negatively modulate the activation of pro-survival AKT proteins thereby resulting in nuclear retention of pro-apoptotic FOXO-1. However, infection leading to sustained inhibition of host cell apoptosis, suggests that FOXO-1 is inactivated despite PD-1-mediated AKT inactivation. Another mechanism by which FOXO-1 may get inactivated despite its nuclear retention is by deacetylation, which also contributes to inhibition of apoptosis (Wang et al., 2014; Yang et al., 2009). Silent information regulator 2 (SIR2) is a NAD-dependent deacetylase that plays a crucial role in the longevity of yeast, worms and flies (Michan and Sinclair, 2007). Mammals express seven homologs of yeast SIR2, identified as the SIRTUIN family, and recent reports suggest that SIRT1 activation may be responsible for prolonging the lifespan in mammals (Cantó and Auwerx, 2009; Salminen et al., 2008). SIRT1-mediated deacetylation of FOXO-1 might contribute to inhibition of apoptosis (Alcendor et al., 2007; Chen et al., 2009; Wang et al., 2013; Yang et al., 2012).

We, therefore, were interested to determine whether *L. donovani* also exploits SIRT1 to escape apoptosis during late phases of infection. We also wanted to have a mechanistic insight into how the parasite might be exploiting PD-1 activation synergistically with the SIRT1/FOXO-1 axis to generate a parasite-conducive environment by suppressing host defense arsenals besides the evasion of host cell apoptosis.
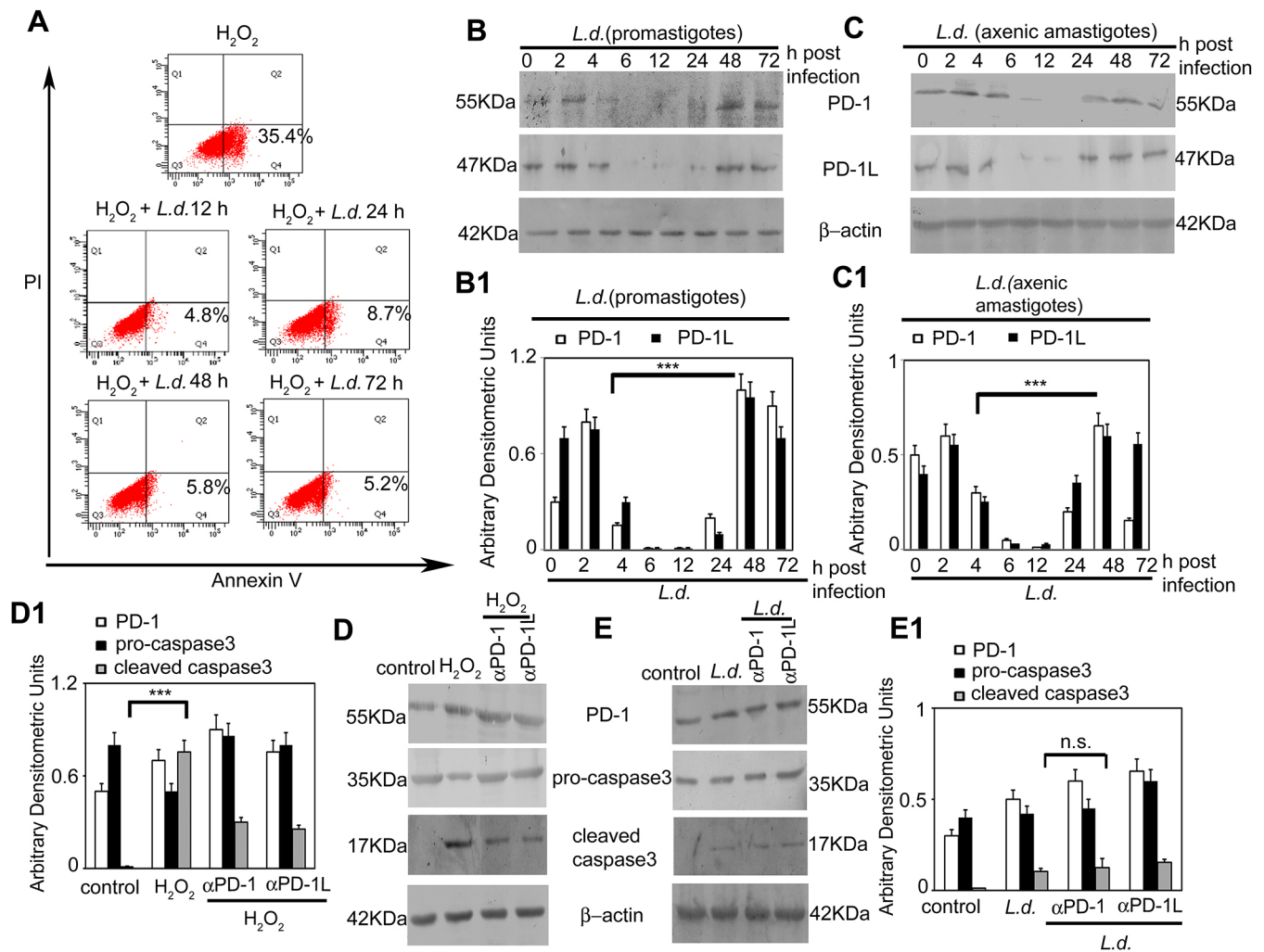
RESULTS

Induction of PD-1 activation in macrophages after *L. donovani* infection without triggering apoptosis

Activation of the PD-1 pathway is related to increased apoptosis of cells (Mühlbauer et al., 2006; Shi et al., 2011) and our previous work documented that during early time points of infection (0–6 h), *L. donovani* downregulates PD-1 expression to inhibit macrophage apoptosis (Roy et al., 2017). However, this was found to be quite the opposite during the late phase of infection (48–72 h). Like what is seen at early time points, *L. donovani* infection also inhibited H_2O_2 (400 µM, 1 h treatment)-induced macrophage apoptosis at late

Fig. 1. Effect of *L. donovani* infection on activation of the PD-1 pathway and macrophage apoptosis. (A) RAW 264.7 macrophages were infected with *L. donovani* (*L.d.*) promastigotes with a parasite:macrophage ratio of 10:1 for the indicated time periods followed by treatment with H_2O_2 (400 μM) for 1 h. Cells were washed and incubated overnight at 37°C and the extent of apoptosis was analyzed by annexin V-FITC–PI flow cytometry. A dual parameter dot plot of FITC fluorescence (*x* axis) versus PI fluorescence (*y* axis) is represented as logarithmic fluorescence intensity. Quadrants represent: lower left, live cells; lower right, apoptotic cells; upper left, necrotic cells; upper right, necrotic or late phase apoptotic cells. (B,C) Macrophages were infected with *L. donovani* promastigotes (B) or axenic amastigotes (C) for different time periods as indicated and expression of PD-1 and PD-1L were evaluated by western blotting with respective antibodies. (D,E) Macrophages incubated with anti-PD-1 or anti-PD-1L antibodies were either treated with H_2O_2 (400 μM) for 1 h (D) or infected with *L. donovani* for 48 h (E). Cells were washed and expressions of pro- and cleaved forms of caspase 3 and PD-1 were monitored by western blotting. Bands were analyzed densitometrically and bar graphs expressing arbitrary densitometric units are presented adjacent to corresponding western blots. Results are mean±s.d. and are representative of three individual experiments (*n*=3). n.s., not significant; ***P<0.001 (Student's *t*-test).

phases (4.8±0.8%, 8.7±2.2%, 5.8±1.0% and 5.2±0.8% at 12 h, 24 h, 48 h and 72 h post infection, respectively, compared, to 35.4± 3.4% in H_2O_2-treated controls, mean±s.d., *P*<0.001) (Fig. 1A). However, unlike what is seen at early time points (6 h), where PD-1 and PD-1L expression considerably decreased starting from 4 h post infection, both showed an increased expression during the late time points with a maximum at 48 h post infection (6.7- and 3.2-fold for PD-1 and PD-1L, respectively, compared to infected cells at 4 h post-infection, *P*<0.001) as observed at up to 72 h post infection (Fig. 1B). A similar result was found upon infection by axenic amastigotes (Fig. 1C). Interestingly, H_2O_2-treated cells, along with increased expression of PD-1 (1.4-fold) (Fig. 1D), also showed a high level of apoptosis (35.4±3.4%) (Fig. 1A). This contradictory observation prompted us to investigate whether PD-1 blockade can influence H_2O_2-induced apoptosis. Treatment with antibodies against either PD-1 or PD-1L significantly decreased the extent of

apoptosis in H_2O_2-treated macrophages, as revealed by decreased cleaved caspase 3 expression (60.0% and 66.7% decrease, respectively; Fig. 1D) and activity (Fig. S1) in H_2O_2-treated macrophages. However, in infected macrophages, there was no detectable change in the cleaved caspase 3 level (Fig. 1E) and caspase 3 activity (Fig. S1) in the presence or absence of PD-1 pathway antagonists at 48 h post infection. All these observations document that *Leishmania*-induced PD-1 expression at late time points has no role in eliciting apoptosis.

Role of PD-1 activation on infection in macrophages

In order to ascertain whether PD-1 pathway activation has any role during the late phase of infection, intra-macrophage parasite survival was measured in the presence of anti-PD-1 antibody. A significant decrease in the number of intracellular amastigotes was noted in anti-PD-1 antibody-treated infected cells (37.9, 30.7 and

37.6% decrease at 48, 72 and 96 h post infection, respectively, compared to the infected control, $P<0.01$), indicating a role for the PD-1 pathway in facilitating parasite survival during the late phase of infection (Fig. 2A). The extent of parasite internalization was found to be similar in both infected and anti-PD-1 antibody-treated infected cells (Fig. 2B). In order to delineate how the PD-1 pathway facilitates parasite survival, we next assessed whether the pathway has any influence on the host-favorable pro-inflammatory cytokines IL-12 and TNFα. Upon PD-1 pathway blockade using anti-PD-1 and anti-PD-1L antibodies, infected macrophages produced significantly increased levels of IL-12 and TNFα (a 3.5- and 4.5-fold increase in TNFα and IL-12 at 48 h post infection, respectively, with respect to infected macrophages, $P<0.001$) (Fig. 2C,D), suggesting that the PD-1 pathway plays a role in downregulating pro-inflammatory cytokine production during infection. Like pro-inflammatory cytokines, infection-induced PD-1 pathway activation also inversely regulated two important antimicrobial defense molecules, namely reactive oxygen species (ROS) and nitric oxide (NO) generation, in the infected macrophages. *L. donovani*-infected macrophages showed a considerable decrease in lipopolysaccharide (LPS)-stimulated ROS and NO levels, which was ameliorated upon PD-1 pathway blockade (2.1- and 4.3-fold increase in ROS and NO, respectively, compared to infected controls, $P<0.001$) as determined by performing an NBT reduction assay and using Griess reagent, respectively (Fig. 2E,F). Taken together, these results suggest that infection-mediated PD-1

pathway induction during late phases of infection plays a role in parasite survival through downregulation of pro-inflammatory cytokines as well as ROS and NO.

Role of PD-1 in mouse model of visceral leishmaniasis
To validate the role of PD-1 signaling in the *in vivo* BALB/c mouse model of visceral leishmaniasis, we treated *L. donovani*-infected mice with antibodies against B7H1 (note herein the alternative name for PD-1L, B7H1, is used to denote experiments performed with antibody from NOVUS Biologicals), which is known to inhibit the PD-1 pathway (Joshi et al., 2009). Dose optimization studies were used to assess the efficacy of anti-B7H1 antibody treatment during a 15-day infection with a dose range of 0–12.5 mg mg/kg body weight/day (Fig. 3A). Infection was allowed to proceed for 6 weeks, after which the anti-leishmanial efficacy was assessed in terms of the parasite burden in the spleen. A maximum inhibition (57.5%) was obtained with a greatly reduced spleen parasite burden at a dose of 5 mg/kg body weight/day (Fig. 3B). The greatly reduced parasite burden was noticed when progression of visceral leishmaniasis was followed in the presence of 5 mg/kg body weight/day anti-B7H1 administered four times at 3 days apart starting at 2 weeks after infection (Fig. 3C). To evaluate the type of immune response in *L. donovani*-infected mice after anti-B7H1 antibody treatment, IL-12 and TNFα levels were determined in isolated splenocytes every 2 weeks after infection with an ELISA. The results demonstrated an
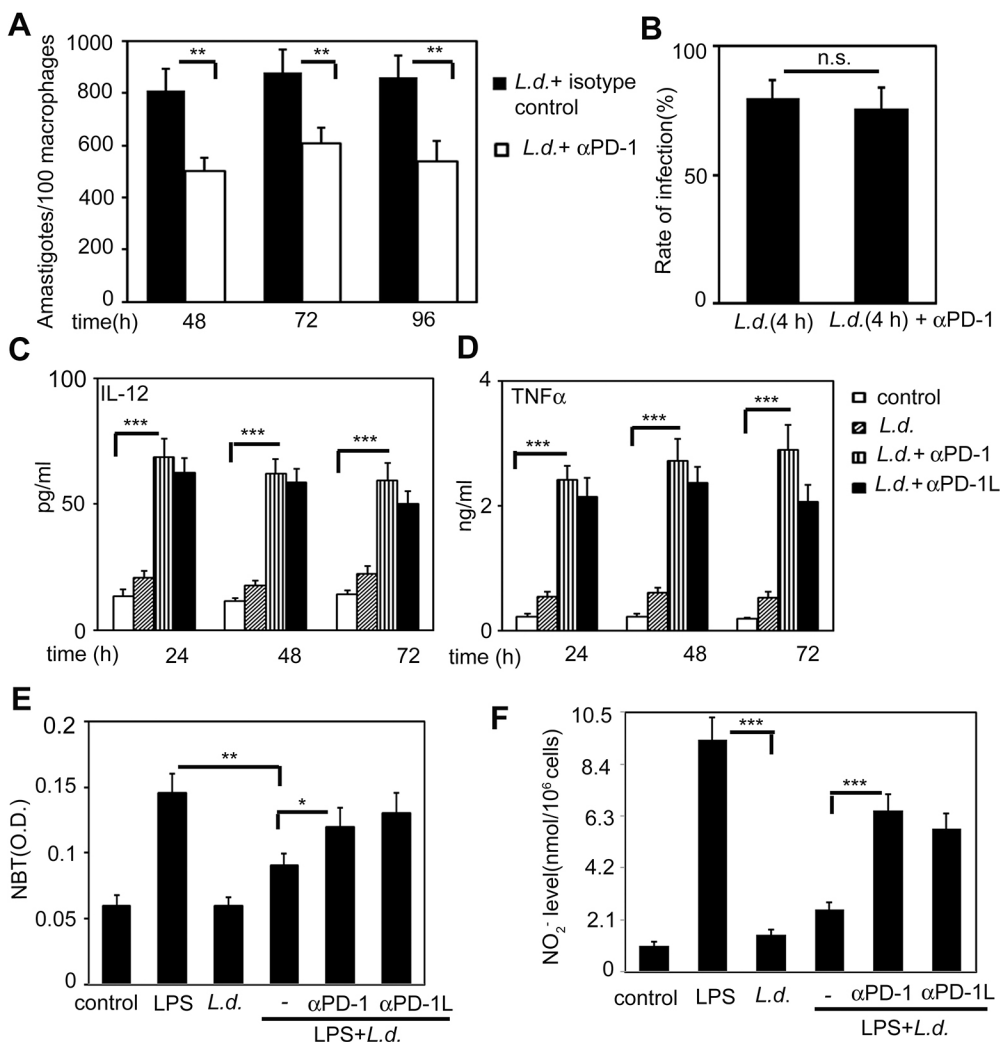
Fig. 2. Effect of *L. donovani*-induced PD-1 pathway activation on parasite survival. (A,B) Macrophages pretreated with anti-PD-1 or control antibody were infected with *L. donovani* (*L.d.*) promastigotes for different time periods as indicated. Intracellular parasite number (A) and rate of infection (B) were determined by Giemsa staining. (C,D) Macrophages incubated with either anti-PD-1 or anti-PD-1L antibodies were infected with *L. donovani* promastigotes for the indicated time periods and secretion of IL-12 (C) and TNFα (D) were estimated by ELISA. (E,F) Cells were incubated with either anti-PD-1 or anti-PD-1L antibodies and infected with *L. donovani* promastigotes for 48 h and harvested. Cells were stimulated with LPS (100 ng/ml) for 30 min before harvest to determine ROS generation through measuring the capacity of macrophages to reduce the NBT level (E) and for 24 h before harvest for measurement of NO level with a Griess reagent assay (F). Results are mean±s.d. and are representative of three individual experiments (*n*=3). n.s., not significant; *$P<0.05$; **$P<0.01$; ***$P<0.001$ (Student's *t*-test).
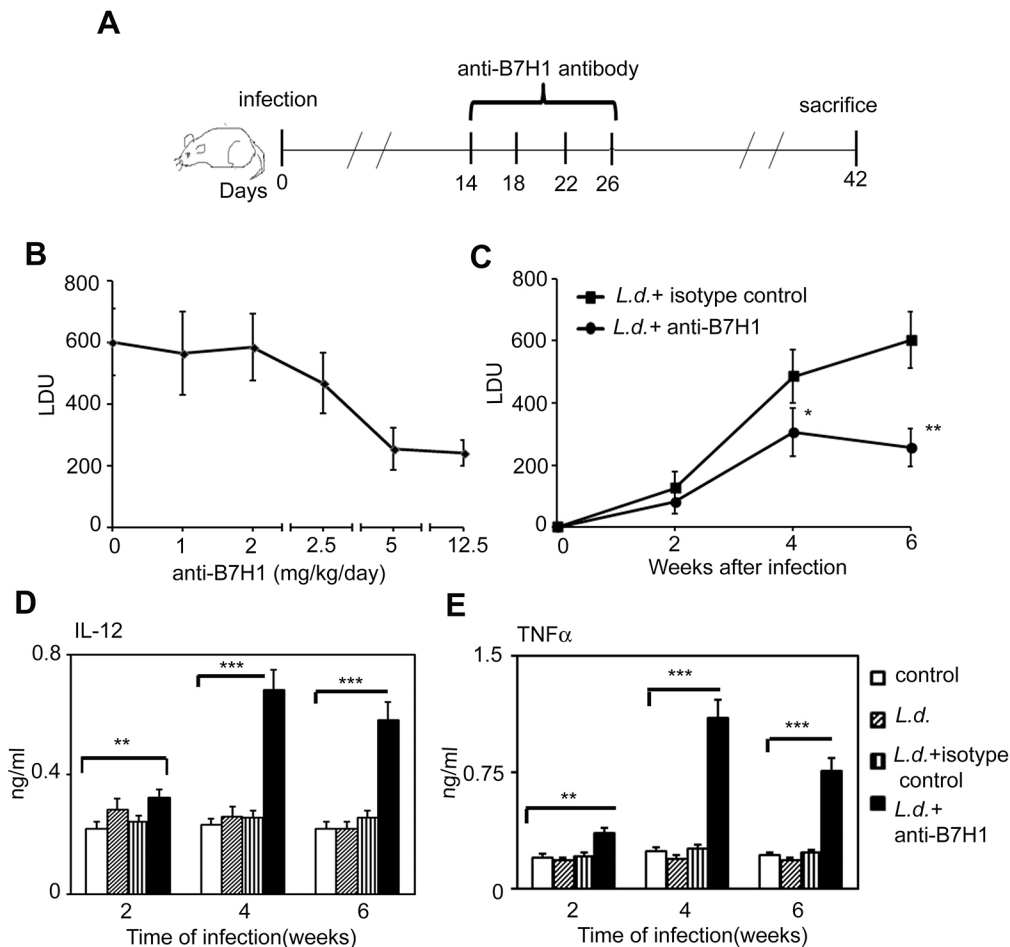
Fig. 3. *In vivo* validation of the role of PD-1 in *L. donovani* infection. (A) Schematic representation of the experimental protocol for treatment of *L. donovani* (*L.d.*)-infected mice with anti-B7H1 antibody. (B) BALB/c mice were infected with 10^7 promastigotes and treated intraperitoneally (i.p.) with various doses of anti-B7H1 antibody (0–12.5 mg/kg body weight/day) given on day 14, 18, 22 and 26. The parasite burden in the spleen was then determined 6 weeks after infection and expressed as the mean±s.d. Leishman–Donovan units (LDU). (C) The course of visceral infection was followed in spleen of mice that had received four i.p. injections of anti-B7H1 antibody (5 mg/kg body weight/day) given on day 14, 18, 22 and 26. (D,E) Splenocytes ($2×10^6$) were isolated from control, infected, and infected plus anti-B7H1 antibody-treated mice at 2, 4, and 6 week post-infection and IL-12 (D) and TNFα (E) levels were determined in culture supernatants via an ELISA. Results are mean±s.d. and are representative of three individual experiments (*n*=3). *P<0.05; **P<0.01; ***P<0.001 (Student's *t*-test).

increased level of IL-12 and TNFα, with a maximum at 4 weeks after infection suggesting an improved host-conducive response in treated mice (Fig. 3D,E). Anti-B7H1 antibody treatment also resulted in marked increase in the content of the major antimicrobial host defense molecules superoxide (O_2^-) and NO in isolated splenocytes with a maximum (2.1- and 2.6-fold, respectively) at 4 weeks after infection (Fig. S2A,B). These results suggest that infection-induced activation of the PD-1 pathway plays a major role in favoring a conducive atmosphere for parasite survival and inhibition of this pathway might have a therapeutic relevance, as it fostered host-protective responses along with suppression of the parasite burden.

Effect of PD-1 activation on AKT and FOXO-1

We previously documented that expression of PD-1, which negatively regulates pro-survival AKT, was downregulated during early *Leishmania* infection, thereby resulting in the inhibition of macrophage apoptosis (Roy et al., 2017). Therefore, it seemed logical to check the status of AKT activation during late phase of *L. donovani* infection where PD-1 expression was found to be upregulated. Kinetic analysis of the level of phosphorylated (p)AKT revealed that although *L. donovani* infection resulted in increased AKT phosphorylation at 6 h post infection (Fig. S3), but no detectable pAKT was observed at 24, 48 and 72 h post infection (Fig. 4A). However, pAKT levels were increased in the infected cells when subjected to anti-PD-1 treatment (Fig. 4A), indicating that AKT phosphorylation is negatively regulated by PD-1. Since the pro-apoptotic transcription factor FOXO-1 is known to be negatively regulated by pAKT (Tzivion et al., 2011; Zhang et al.,

2011), we checked the status of FOXO-1. Analysis of FOXO-1 levels by western blotting in both cytosolic and nuclear fractions of infected macrophages at 24, 48 and 72 h post infection revealed that it was mostly localized in the nuclear fractions (Fig. 4B), and treatment with anti-PD-1 antibody significantly decreased nuclear FOXO-1 levels (Fig. 4C). Consistent with the western blot analysis, microscopy experiments with FITC-labeled FOXO-1 showed that it had a maximum nuclear localization at 48 h post infection, as documented by the number of colocalizing DAPI- and FITC-positive pixels (Fig. 4D). In order to ascertain why apoptosis was inhibited in spite of nuclear retention of FOXO-1, cells were transfected with either wild-type (WT)-FOXO-1 or constitutively active (CA)-FOXO-1, infected with *L. donovani*, subjected to H_2O_2 treatment and assessed for caspase 3 activity (Fig. 4E). Transfection efficiency was monitored by the expression of GFP in whole-cell lysates of transfected cells through western blot analysis (Fig. 4E, inset). Although in both cases, FOXO-1 was found to be localized in nucleus (data not shown), CA-FOXO-1 led to a significantly increased activity of caspase 3 compared to WT-FOXO-1-transfected infected cells thereby suggesting that apart from nuclear retention, that FOXO-1 needs additional activation to induce apoptosis at late phase of infection (Fig. 4E). A significant decrease in the number of intracellular amastigotes was noted in CA-FOXO-1 transfected cells (42.1%, 41.5% and 42.5% decrease at 48, 72 and 96 h post infection, respectively, compared to what was seen in WT-FOXO-1-transfected cells, *P*<0.01) (Fig. 4F), further justifying the requirement for FOXO-1 inactivation during infection. Taken together, these results indicate that although AKT is deactivated during the late phases of infection, leading to increased
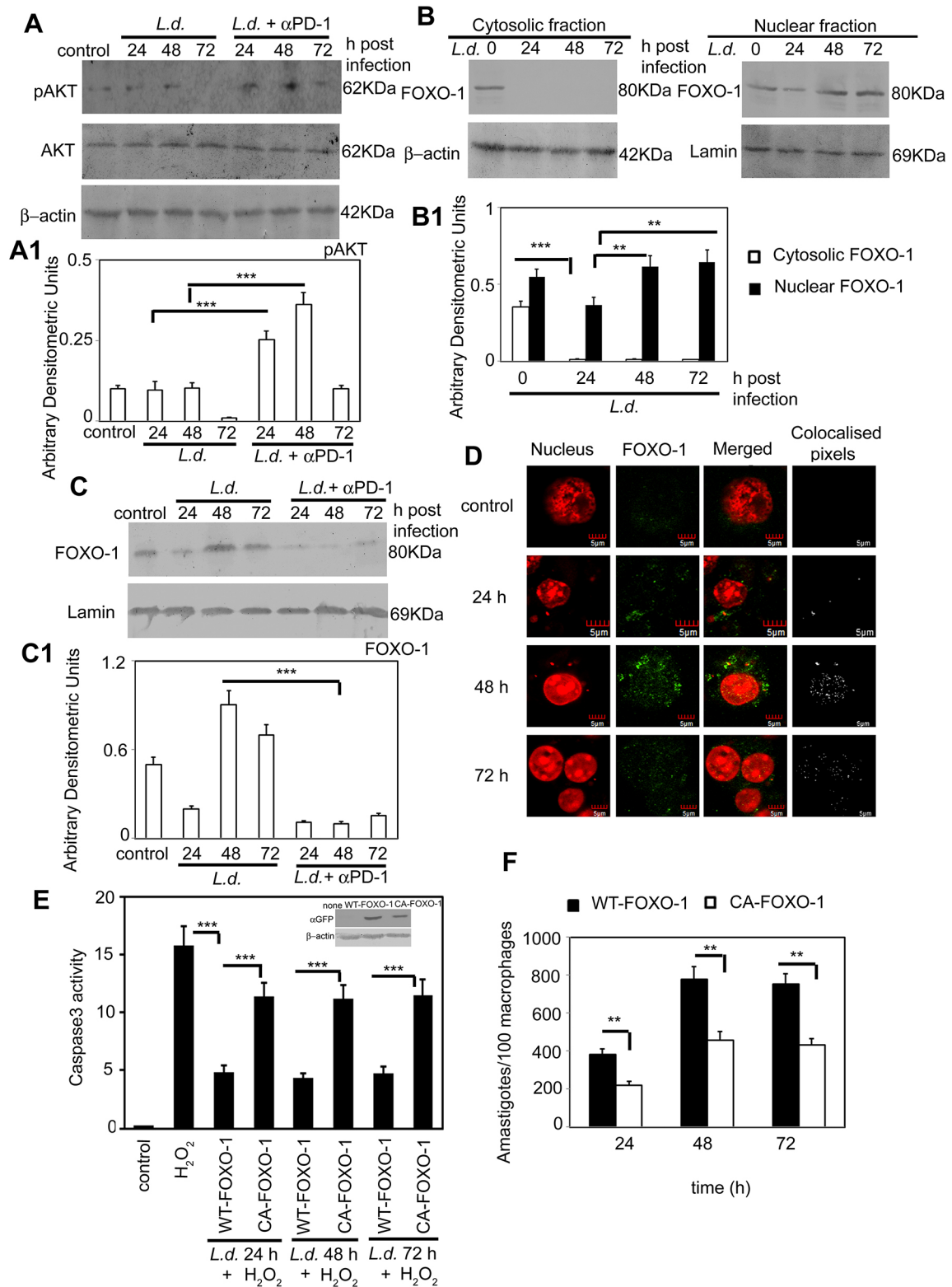
Fig. 4. See next page for legend.

nuclear retention of FOXO-1, nuclear FOXO-1 is not active to induce apoptosis.

Role of SIRT1 on infection-induced inactivation of FOXO-1

The inability of nuclear FOXO-1 to activate apoptosis might be because of its deacetylation, as deacetylated FOXO cannot act as an

apoptotic transcription factor (Wang et al., 2014; Yang et al., 2009; Zhang et al., 2011). To determine the status of FOXO-1, it was immunoprecipitated from the nuclear lysates of infected macrophages and probed with anti-pan-acetyl lysine antibody. No detectable level of acetylation was observed in 24, 48 and 72 h infected cells, indicating that FOXO-1 is mostly in the deacetylated

Fig. 4. Effect of *L. donovani* infection on AKT and FOXO-1.
(A) Macrophages were incubated with anti-PD-1 antibody and subjected to infection with *L. donovani* (*L.d.*) promastigotes for the indicated time periods, and levels of pAKT and total AKT were monitored by western blotting. (B) Nuclear and cytosolic fractions were isolated from cells infected for indicated time periods and then expression of FOXO-1 was analyzed by western blotting. (C) Cells were incubated with anti-PD-1 antibody and infected for the indicated time periods and then expression of FOXO-1 was analyzed by western blotting in nuclear fractions. (D) Macrophages were infected with *L. donovani* promastigotes for indicated time periods, and treated with anti-FOXO-1 monoclonal antibody followed by FITC-conjugated secondary antibody. Nuclei were stained with DAPI and cells were analyzed under a microscope. Images were analyzed for colocalization using Olympus Fluoview (version 3.1a; Tokyo, Japan). For better visualization, red was used instead of blue to mark DAPI using the LUT program of Fluoview. Green or yellow colors on a red nucleus denote strong colocalization, whereas a red nucleus lacking any green or yellow colors denotes exclusion. (E) Macrophages were transfected with WT- or CA-FOXO-1 expression plasmids (24 h) and then infected with *L. donovani* promastigotes for indicated time periods followed by treatment with H_2O_2 (400 μM) for 1 h. Total cellular extracts (10 μg of protein per sample) were used to determine caspase 3 activity using Ac-DEVD-pNA as a substrate. Inset, confirmation that the plasmids were expressed. (F) Cells were transiently transfected with WT- or CA-FOXO-1 expression plasmids, followed by infection with *L. donovani* promastigotes for indicated time periods. Intracellular amastigote number was determined by Giemsa staining. Bands were analyzed densitometrically and bar graphs expressing arbitrary densitometric units are presented adjacent to corresponding western blots. Results are mean±s.d. and are representative of three individual experiments (*n*=3). **P<0.01; ***P<0.001 (Student's *t*-test).

state (Fig. 5A). Since SIRT1-mediated FOXO-1 deacetylation plays a major role in inhibition of apoptosis (Alcendor et al., 2007; Chen et al., 2009; Wang et al., 2013), we therefore examined whether *L. donovani* infection modulates SIRT1 expression in infected macrophages. Kinetic analysis revealed an increased SIRT1 expression in infection, with the maximum level obtained at 48 h post infection (3-fold, *P*<0.001) as observed at up to 72 h post infection (Fig. 5B). Next, to find out whether SIRT1 plays any role in the inactivation of FOXO-1, we silenced SIRT1 expression in infected RAW264.7 macrophages through treatment with SIRT1 siRNA and monitored the acetylation state of FOXO-1 in the nuclear lysates. The knockdown efficiency was found to be 88.2% as determined by western blotting (data not shown). Marked acetylation of FOXO-1 was observed in the SIRT1-knockdown infected cells, which validates the involvement of SIRT1 in deacetylation of FOXO (Fig. 5C). Significant acetylation of FOXO-1 was also observed in the infected macrophages treated with sirtinol (50 μM, 48 h), a SIRT1 inhibitor (Fig. S4A), confirming the role of SIRT1 in mediating FOXO-1 deacetylation.

To ascertain whether SIRT1-mediated deacetylation of FOXO-1 has any impact on its nuclear retention, localization of FOXO-1 was monitored in SIRT1 siRNA-treated infected cells. Silencing of SIRT1 did not alter the nuclear localization of FOXO-1 in infected cells, as evident from microscopic experiments with FITC-conjugated anti-FOXO-1 antibody (Fig. 5D). Western blot analysis also corroborated the observation (Fig. S4B). Furthermore, to ascertain whether the physical interaction between SIRT1 and FOXO-1 is necessary to mediate FOXO-1 deacetylation, co-immunoprecipitation and reciprocal co-immunoprecipitation studies were performed using the nuclear fraction of infected cells and anti-FOXO-1 and anti-SIRT1 antibodies, respectively. An increased association of SIRT1 with FOXO-1 was noted in nuclear extracts isolated from infected cells upon FOXO-1 immunoprecipitation and blotting with anti-SIRT1 antibody (data not shown). Likewise, a significantly increased association was also

observed upon SIRT1 immunoprecipitation and blotting with anti-FOXO-1 antibody, suggesting that SIRT1 interacts with FOXO-1 in the nucleus (Fig. 5E). Next, to find out whether SIRT1-mediated deacetylation of FOXO-1 is associated with inhibition of apoptosis, the extent of apoptosis was evaluated in sirtinol-treated infected macrophages through both annexin V–propidium iodide (PI) flow cytometry analysis and a caspase 3 activity assay (Fig. 5F; Fig. S4C). The inhibition of apoptosis in *L. donovani*-infected cells was markedly rescued by sirtinol treatment, which again decreased significantly when FOXO-1 inhibitor was co-administered with sirtinol in infected macrophages (Fig. 5F). These findings were further validated by the caspase 3 activity assay (Fig. S4C), thereby indicating that SIRT1-dependent deacetylation-mediated inactivation of FOXO-1 is responsible for the inhibition of apoptosis in infected cells.

Leishmania deploy the SIRT1/FOXO-1 axis to foster a parasite-conducive environment along with mediating the evasion of host apoptosis

In order to assess the contribution of SIRT1 in parasite survival, intracellular parasite numbers were assessed in SIRT1-silenced RAW macrophages, which led to markedly decreased parasite survival (73.7% decrease compared to the control siRNA-transfected macrophages, *P*<0.001) (Fig. 6A). Sirtinol also significantly decreased the intracellular amastigote count with a maximum inhibition at 50 μM (Fig. 6B). The rate of infection was unaltered in siRNA- or sirtinol-treated macrophages as studied after 4 h infection (data not shown). Interestingly, sirtinol treatment in WT-FOXO-1-transfected infected cells led to a significant decrease in the intracellular parasite count, which was reversed in the presence of FOXO-1 inhibitor, suggesting that the SIRT1-mediated effects are FOXO-1 dependent (Fig. 6C). In contrast, there was no inhibitory effect of sirtinol in CA-FOXO-1-transfected cells intracellular parasite count (Fig. 6C), further validating the hierarchy of SIRT1/FOXO-1 axis. Since SIRT1 is known to have an anti-inflammatory role (Yoshizaki et al., 2009), we assessed the impact of expressing CA-FOXO-1 (which is in its acetylated form) on LPS-induced TNFα secretion. As shown in Fig. 6D, cells expressing CA-FOXO-1 showed enhanced TNFα secretion as compared to WT-FOXO-1-transfected infected cells. However, administration of sirtinol in the WT-FOXO-1-transfected infected macrophages significantly increased the LPS-induced TNFα secretion (2.5-fold with respect to infected cells, *P*<0.001) which was reversed by co-treatment with FOXO-1 inhibitor (55.03% decrease compared to sirtinol-treated cells, *P*<0.01) indicating that FOXO-1 may be operating downstream of SIRT1 in modulating TNFα production (Fig. 6D). Similarly, WT-FOXO-1-transfected infected cells showed a decrease in LPS-stimulated ROS levels, which was reversed by sirtinol treatment. However, co-administration of FOXO-1 inhibitor with sirtinol in the infected cells transfected with WT-FOXO-1 resulted in the abrogation of the sirtinol-mediated increase in ROS generation (Fig. 6D), validating the role of SIRT1/FOXO-1 axis in suppressing ROS generation. A similar effect was seen for NO generation in infected cells (Fig. 6E). Taken together, these results suggest that *L. donovani* exploits the SIRT1/FOXO-1 axis of host macrophages to foster parasite survival through inhibition of apoptosis and generation of antimicrobial arsenals.

Role of SIRT1 in BALB/c mouse model of visceral leishmaniasis
In order to assess the role of SIRT1 in the in vivo BALB/c mouse model of visceral leishmaniasis, we infected mice with *L. donovani*
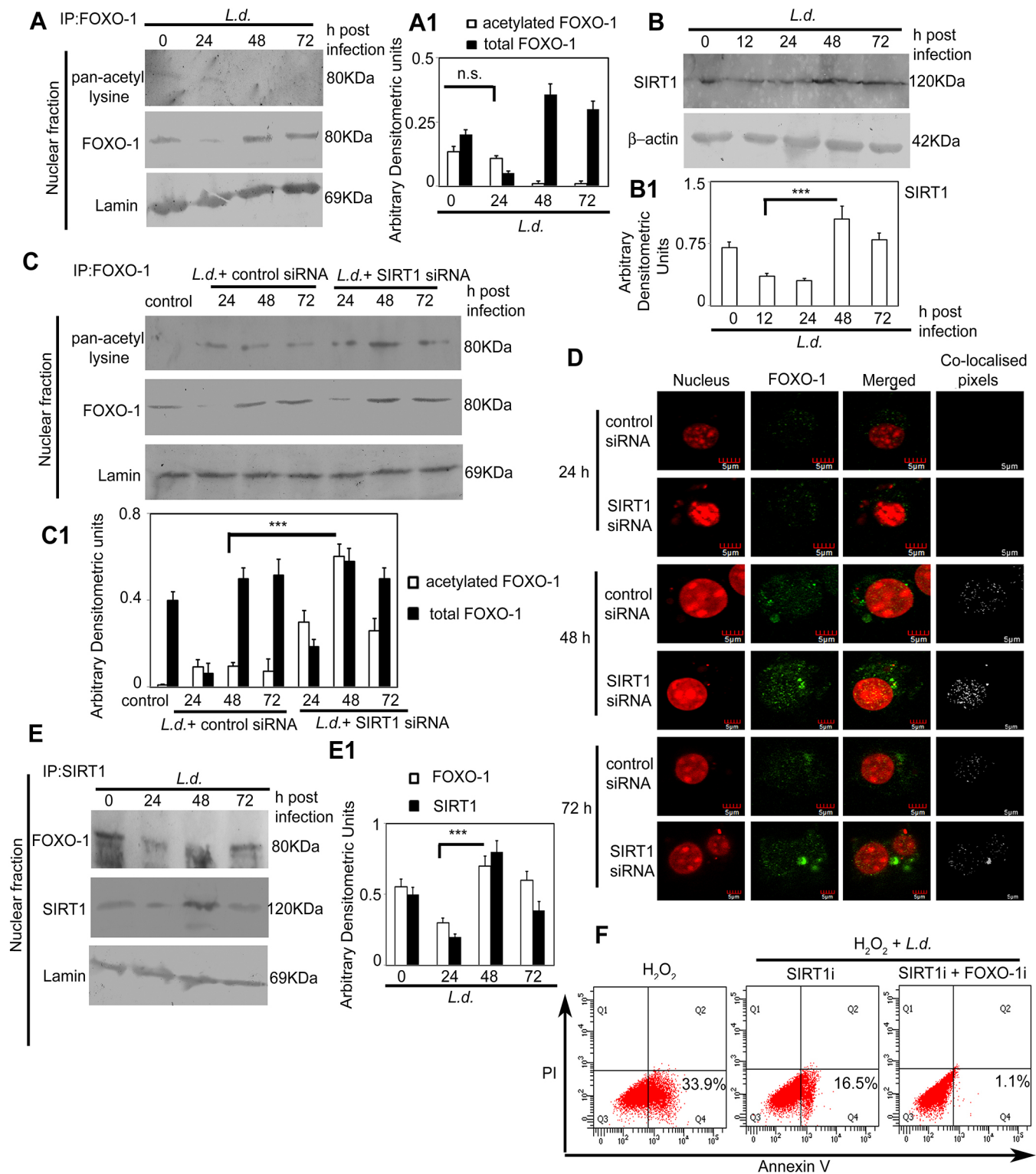
Fig. 5. See next page for legend.

for 15 days and administered sirtinol intraperitoneally twice a week for 4 weeks. Then the spleen parasite burden was assessed after 6 weeks of infection. Dose optimization studies revealed the maximum suppression (63.4% decrease) of parasite burden occurred at a dose of 10 mg/kg body weight/day (Fig. 7A). Progression of visceral leishmaniasis in the presence of sirtinol at 10 mg/kg body weight/day was also monitored and a substantial

reduction in spleen parasite burden was observed (Fig. 7B). To evaluate the impact of SIRT1 inhibition on the host-protective pro-inflammatory environment, TNFα was measured in the supernatants of splenocytes isolated from sirtinol-treated infected mice, which resulted in significant increase with a maximum at 4 weeks post infection (3.6-fold increase compared to vehicle-treated control, $P<0.001$) (Fig. 7C). Furthermore, a significant increase in

Fig. 5. The role of SIRT1 on deacetylation of FOXO-1 during *L. donovani* infection. (A) Cells were infected with *L. donovani* (*L.d.*) promastigotes for the indicated time periods. Nuclear lysates were prepared and nuclear extracts were immunoprecipitated (IP) with anti-FOXO-1 antibody and then subjected to immunoblotting with pan-acetyl-lysine antibody. (B) Cells were infected for indicated time periods and expression of SIRT1 was evaluated by western blotting. (C) Cells were transfected with control or SIRT1 siRNA followed by infection with *L. donovani* promastigotes for indicated time periods. Nuclear lysates prepared from infected cells were immunoprecipitated with anti-FOXO-1 antibody and then subjected to immunoblotting with pan-acetyl-lysine antibody. (D) Cells were transfected with control or SIRT1 siRNA followed by infection with *L. donovani* promastigotes for indicated time periods, stained with anti-FOXO-1 monoclonal antibody followed by FITC-conjugated secondary antibody. Nuclei were stained with DAPI and cells were analyzed as described in Fig. 4D. (E) Macrophages were infected for the indicated time periods and nuclear fractions were prepared. Nuclear lysates from infected macrophages were immunoprecipitated with anti-SIRT1 antibody and then the expression of FOXO-1 and SIRT1 was analyzed by western blotting with the respective antibodies. (F) Macrophages were treated with sirtinol (SIRT1i; 50 μM) alone or with FOXO-1 inhibitor (FOXO-1i; 50 nM) followed by infection with *L. donovani* promastigotes for 48 h and treatment with H_2O_2 (400 μM) for 1 h. Cells were washed and incubated overnight at 37°C and the extent of apoptosis was analyzed by annexin V-tagged FITC–PI flow cytometry. Bands were analyzed densitometrically and bar graphs expressing arbitrary densitometric units are presented adjacent to corresponding western blots. Results are mean±s.d. and are representative of three individual experiments (*n*=3). n.s., not significant; ***$P<0.001$ (Student's *t*-test).

superoxide and NO levels was observed in splenocytes from sirtinol-treated infected mice (Fig. 7D,E). Moreover, co-administration of anti-B7H1 antibody (5 mg/kg body weight/day) along with sirtinol (10 mg/kg body weight/day) led to enhanced suppression (84.7% decrease) of parasite burden compared to the treatments with anti-B7H1 antibody or sirtinol alone (Fig. 7F). Collectively, these results highlight the anti-leishmanial efficacy of sirtinol, and the synergistic influence of anti-B7H1 antibody when used combinatorially with sirtinol.

DISCUSSION

Previously, we showed that the macrophage PD-1 receptor plays a major role in apoptosis and that the early phase of *Leishmania* infection downregulates PD-1, thus inhibiting apoptosis and facilitating parasite survival (Roy et al., 2017). However, in the present study, we showed that during late phase of infection, in spite of upregulation of both PD-1 receptor and PD-1 ligand, apoptosis of macrophages was still markedly inhibited. We tried to elucidate the underlying mechanism and observed that PD-1 activation resulted in deactivation of AKT coupled with the sequestration of FOXO-1 in the nucleus, which should have facilitated apoptosis. However, FOXO-1 was in its inactive deacetylated state and hence did not contribute to apoptosis. We also identified that infection upregulated the expression of SIRT1, a potential candidate responsible for FOXO-1 deacetylation (Fig. 8). Inhibitor-based approaches as well as genetically silencing experiments substantiated the role of SIRT1 in mediating deacetylation of nuclear FOXO-1, thereby resulting in inhibition of apoptosis. Furthermore, we also showed that, apart from the suppression of host cell apoptosis, the parasite deployed the SIRT1/FOXO-1 axis to facilitate its survival through negative modulation of host-antimicrobial arsenals such as pro-inflammatory cytokines and reactive oxygen and nitrogen species.

Increased PD-1 expression during late infection did not correspondingly correlate with increased apoptosis of infected cells, which suggested that there could be an apoptosis-independent effect for PD-1. Unlike H_2O_2-mediated PD-1 induction, infection-induced PD-1 upregulation did not lead to enhanced apoptosis. Blockade of PD-1 receptor resulted in decreased parasite survival and ameliorated the secretion of the pro-inflammatory cytokines IL-12 and TNFα, together with enhancing the production of host defense ROS and NO molecules. This indicates that PD-1 pathway activation in the late phase of infection plays a role in producing a congenial environment for the parasite by curbing generation of ROS, NO and pro-inflammatory cytokines. This is in agreement with the finding that in case of chronic infection by hepatitis C virus, PD-1 dampens IL-12 expression in monocytes/macrophages, thereby suggesting an anti-inflammatory role for PD-1 (Ma et al., 2011). Moreover, PD-1 engagement with its agonist leads to inhibition of iNOS and TNFα expression in macrophages (Chen et al., 2016), further supporting the idea that PD-1 has an anti-inflammatory role.

The present study showed that PD-1 pathway activation negatively regulates AKT activation in macrophages, which is in line with a report stating no significant AKT activation occurs during *L. donovani* infection (Dey et al., 2007). The present study also demonstrated that nuclear retention of FOXO-1 during the late phases of infection was mediated by the PD-1 pathway, thus confirming a reciprocal relationship between AKT activation and FOXO-1 retention. However, the reason why the increased nuclear FOXO-1 did not culminate in increased apoptosis was not delineated and, here, we found that FOXO-1 was primarily in its deacetylated state and hence could not induce apoptosis. This is in agreement with several reports that indicate that, upon deacetylation, FOXO-1 cannot trigger apoptosis (Chen et al., 2009; Wang et al., 2013, 2014; Yang et al., 2009). SIRT1 was then identified as the major player for mediating deacetylation of FOXO-1 resulting in inhibition of apoptosis. Increased SIRT1 expression during the late phase of infection and the evidence that SIRT1 knockdown and SIRT1 inhibition both rendered FOXO-1 into an acetylated state further confirmed our notion. Moreover, we noticed that SIRT1 knockdown and SIRT1 inhibition with the pharmacologic inhibitor sirtinol both led to reduced parasite survival, further corroborating its role in parasite survival. Moreover, we also delineated that *Leishmania* exploits the SIRT1/FOXO-1 axis to negatively regulate inflammatory TNFα production, ROS generation and NO production. This idea is supported by reports suggesting that SIRT1 has a potential anti-inflammatory role (Winnik et al., 2012; Yang et al., 2012; Yoshizaki et al., 2009). However, the present study emphasized a relatively new mechanism behind the SIRT1-mediated negative modulation of inflammatory response involving the SIRT1/FOXO-1 route that is different from the underlying mechanisms documented previously. Although the mechanism of apoptosis-evasion deployed by *L. donovani* during early phase of infection has been shown to be mediated by downregulation of PD-1 (Roy et al., 2017), the present study focuses on a novel mode of escape from apoptosis involving the crosstalk of the longevity factor SIRT1 with the death receptor PD-1 activated during the late phase of infection.

MATERIALS AND METHODS
Chemicals and reagents

Protease inhibitors, bovine serum albumin (BSA), 5 bromo-4-chloro-3′ indolyphosphate (BCIP) and mouse monoclonal β-actin antibody (1:5000, cat. no. A2228-200UL, Sigma) were obtained from Sigma-Aldrich (St Louis, MO). Penicillin G and streptomycin solution, Dulbecco's modified Eagle's medium (DMEM), RPMI 1640, M199, recombinant human granulocyte-macrophage colony-stimulating factor (GM-CSF) and fetal bovine serum (FBS) were obtained from Invitrogen (Carlsbad, CA).
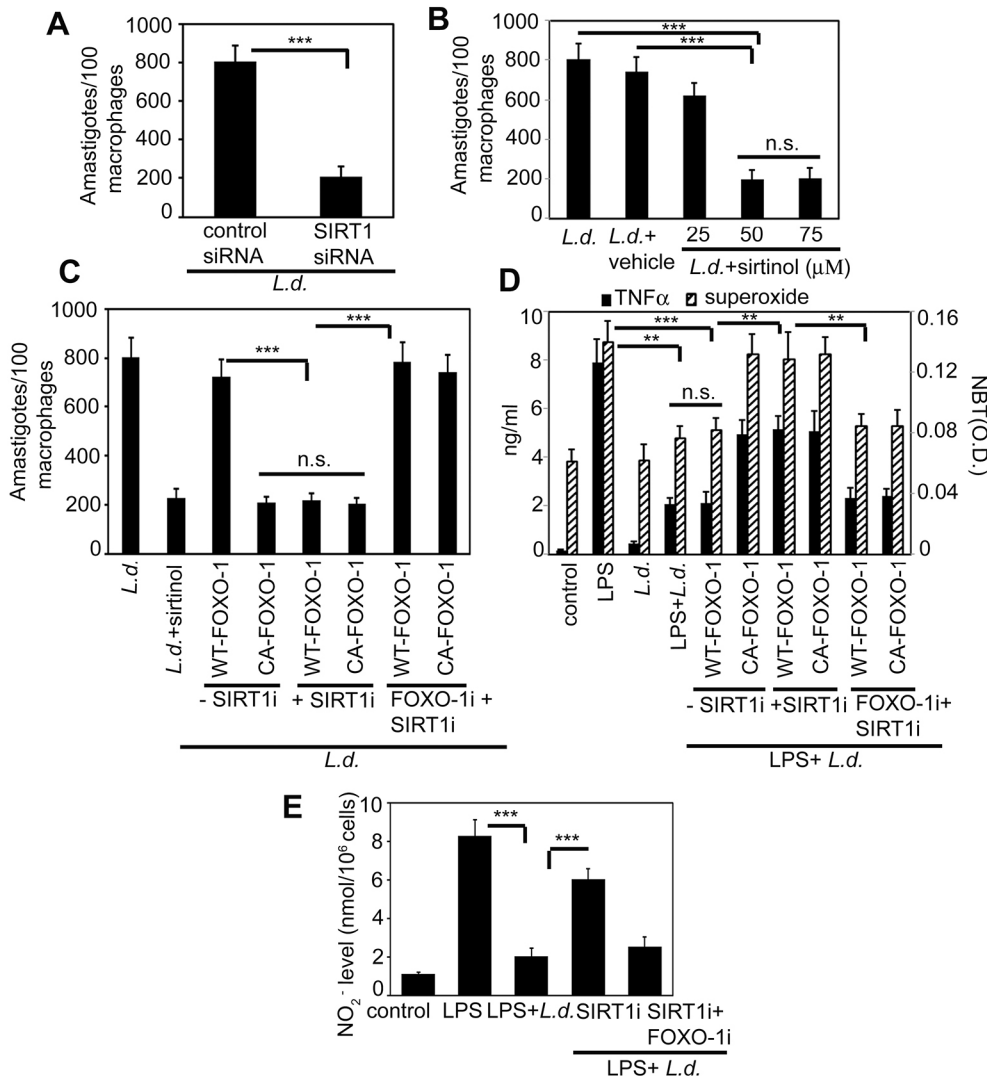
Fig. 6. Role of SIRT1 and FOXO-1 in modulation of inflammatory responses and parasite survival. (A,B) Macrophages were transfected with control or SIRT1 siRNA (A) or incubated with increasing concentrations (0–75 μM) of sirtinol (B) and infected with *L. donovani* (*L.d.*) promastigotes for 48 h. Intracellular parasite number was determined by Giemsa staining. (C,D) Macrophages were transfected with WT- or CA-FOXO-1 expression plasmids (24 h), followed by infection with *L. donovani* promastigotes for 48 h and treatment with sirtinol alone or co-treatment with sirtinol and FOXO-1 inhibitor. Intracellular parasite numbers were measured by Giemsa staining (C) and generation of TNFα was estimated by ELISA (D) after stimulation with LPS (100 ng/ml). (E) Cells treated with sirtinol (SIRT1i) alone or co-treated with FOXO-1 inhibitor (FOXO-1i) were infected with *L. donovani* promastigotes for 48 h. Cells were stimulated with LPS (100 ng/ml) for 24 h and NO level was measured by the Griess reagent assay. Results are mean± s.d. and are representative of three individual experiments (*n*=3). n.s., not significant; **P<0.01; ***P<0.001 (Student's *t*-test).

Antibodies against AKT (1:2000, CST-9271) and pAKT (1:2000, CST-9272) were obtained from Cell Signaling Technology (Danvers, MA). Mouse monoclonal antibodies against PD-1 (1:1000, sc-73402, RMP1-14), PD-1L1 (1:1000, sc-50298, H130), FOXO-1 (1:1000, sc-374427, C-9), SIRT1 (1:1000, sc-15404, H-300), pan-acetyl-lysine (1:1000, sc-8649, C2) and lamin A (1:1000, sc-6214, C-20), protein A/G plus agarose beads, SIRT1 siRNA (sc-40987), control siRNA (sc-37007), alkaline phosphatase (AP)-conjugated anti-mouse-IgG (1:5000, sc-3698), anti-rabbit-IgG (1:5000, sc-3838) and anti-goat-IgG (1:5000, sc-2022), and FITC-conjugated anti-mouse-IgG (1:100, sc-2010) secondary antibodies were obtained from Santa Cruz Biotechnology (Santa Cruz, CA). Sirtinol, the FOXO-1 inhibitor AS1842856 (FOXO-1i) and NBT were from Calbiochem (San Diego, CA). The annexin-V FLUOS staining kit was purchased from Roche Applied Science (Indianapolis, IN). Anti-B7H1 antibody (100 μg of antibody per mouse i.p. injection, M1H5, NBP1-43262) was purchased from NOVUS Biologicals (Littleton, CO). Recombinant PD-1L1-Ig chimera was obtained from R&D Systems (Minneapolis, MN). WT-FOXO-1 (GFP-FOXO-1) and CA-FOXO-1 (FOXO-1-ADA-GFP) were Addgene plasmids #17551 and 35640 (deposited by Domenico Accili).

Cell culture and parasite maintenance

The murine macrophage cell line RAW264.7 was cultured at 37°C with 5% CO2 in RPMI 1640 supplemented with 10% heat-inactivated FBS, 100 μg/ml streptomycin and 100 U/ml penicillin. The promastigotes of *L. donovani* strain (MHOM/IN/1983/AG83) were maintained in Medium 199 supplemented with 10% fetal calf serum, 50 U/ml penicillin and 50 μg/ml streptomycin. *In vitro* infection experiments were carried out with RAW 264.7 cell line (National Repository for Cell lines/Hybridomas, Department of Biotechnology, Govt. of India) using stationary phase promastigotes at a 10:1 parasite:macrophage ratio. *L. donovani* axenic amastigotes were cultured as described previously (Ghosh et al., 2013). For *in vivo* infection, 10^7 *L. donovani* promastigotes were injected via the tail vein of female BALB/c mice. Parasite burdens were ascertained by Giemsa-stained impression smears of spleen isolated from infected mice. Spleen parasite burden was expressed as Leishman–Donovan units (LDU) and were calculated as the number of amastigotes/1000 nucleated cells×organ weight (in grams) (Kar et al., 2010). Animal care and experimental procedures were carried out in accordance with the recommendations in the Guide for the Care and Use of Laboratory Animals of the National Institutes of Health. The protocol has been approved by the Committee on the Ethics of Animal Experiments of Indian Institute of Chemical Biology (permit number 147-1999).

PD-1 pathway blockade

During *in vitro* blockade experiments, macrophages incubated with anti-PD-1 or anti-PD-1L antibodies were infected with *L. donovani* parasites for the indicated time periods. For *in vivo* infection, anti-mouse PD-1L1/B7H1 monoclonal antibody (0–12.5 mg/kg body weight) was administered intraperitoneally four times 3 days apart starting at 2 weeks post infection. Rat IgG (R&D Systems) was used as isotype control. Before treatment, antibodies were tested for functionally relevant LPS contamination by
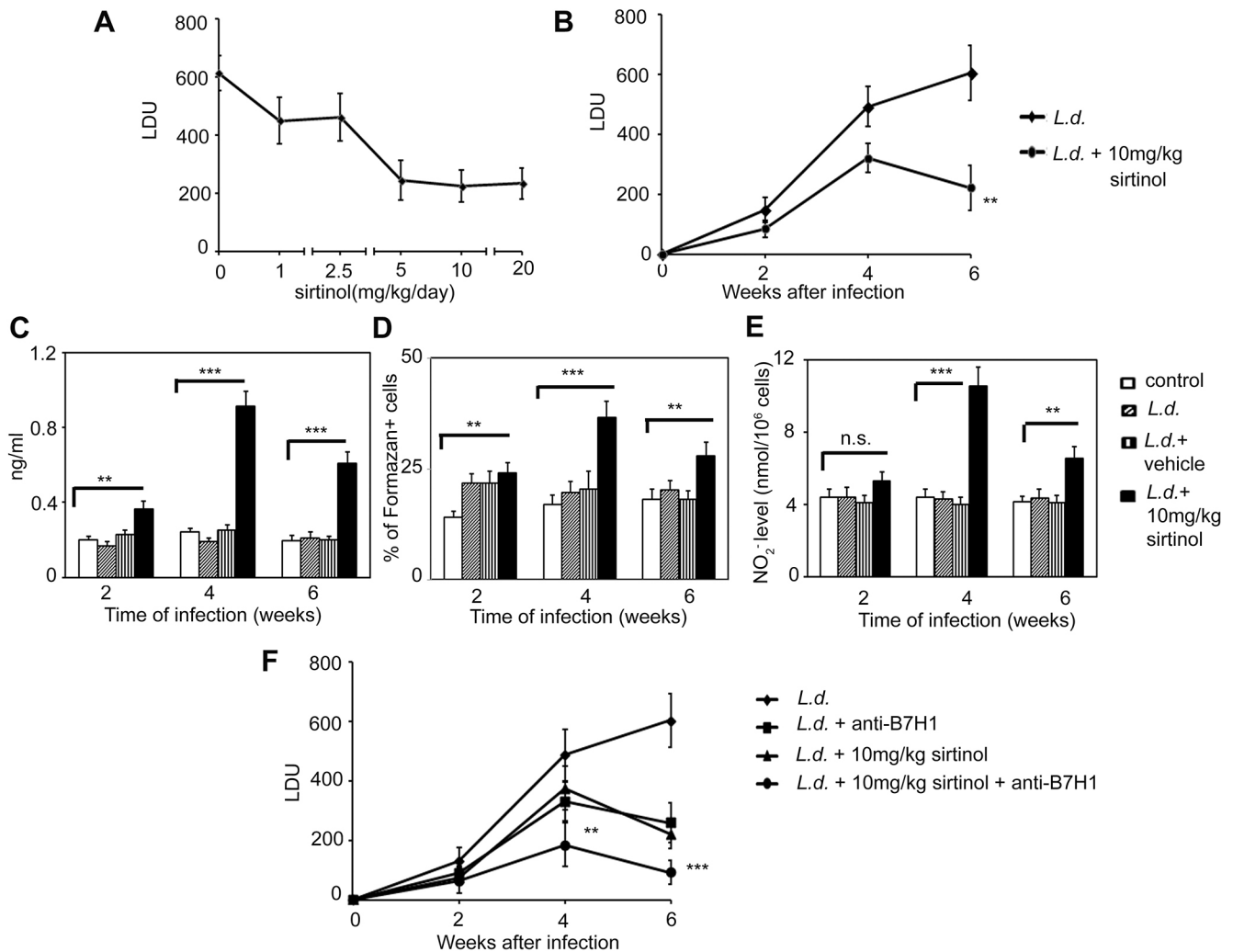
Fig. 7. *In vivo* validation of the role of SIRT1 in *L. donovani* infection. (A) BALB/c mice were infected with 10^7 promastigotes and treated intraperitoneally (i.p.) with various doses of sirtinol (0–20 mg/kg body weight/day) given twice weekly for 4 weeks starting at 2 weeks post infection. The parasite burdens in spleen were then determined 6 weeks after infection. (B) The progression of visceral infection was determined in BALB/c mice that had received i.p. injections of sirtinol (10 mg/kg body weight/day) twice weekly for 4 weeks starting at 2 weeks after infection. (C–E) Splenocytes ($2×10^6$) were isolated from control, infected and infected plus sirtinol-treated mice at 2, 4 and 6 weeks post-infection. The TNFα level was determined in culture supernatants by ELISA (C). The superoxide content of cells was assessed by NBT assay (D) and the NO level was measured by the Griess reagent assay (E) after incubation with 5 µg of soluble leishmanial antigen at 37°C for 48 h. (F) The progression of visceral infection at various time periods post infection was followed in spleen of mice that had received sirtinol (10 mg/kg body weight/day) i.p. alone or in combination with anti-B7H1 antibody (5 mg/kg body weight/day). Results are mean±s.d. and are representative of three individual experiments (n=3). n.s., not significant; **$P<0.01$; ***$P<0.001$ (Student's t-test).

assaying their ability to synergize with IFNγ, for the induction of inducible NO synthase (Joshi et al., 2009). No activity was detectable in those assays (sensitivity, 1 ng/ml LPS; data not shown).

Apoptosis detection by annexin V staining
RAW 264.7 cells ($2×10^6$) were infected with *L. donovani* promastigotes for different time periods. One group of infected macrophages for each time point of infection was treated with H_2O_2 for 1 h; then, culture medium was replaced and cells were incubated overnight at 37°C/5% CO_2. Cells were washed twice with PBS. Apoptosis was then determined using annexin-V FLUOS staining kit as per the manufacturer's instruction. Cells were analyzed on FACS BD LSR FORTESSA machine using 488 nm excitation and 530 nm emission for FITC and >600 nm for PI fluorescence using FACS Diva software.

Immunoprecipitation and immunoblotting
Cells were lysed in lysis buffer (Cell Signaling Technology), and the protein concentrations in the cleared supernatants were estimated using a Bio-Rad protein assay (Bio-Rad). Immunoprecipitation was performed as described

previously (Roy et al., 2017). Briefly, pre-cleared cell lysates (500 µg) were incubated overnight with specific primary antibody at 4°C. 25 µl of Protein A/G plus agarose beads were added to the mixture and incubated for 4 h at 4°C. Immune complexes were collected and washed three times with ice-cold lysis buffer and once with lysis buffer without Triton X-100. The immunoprecipitated samples and cell lysates were resolved by 10% SDS-PAGE and then transferred onto nitrocellulose membrane (Millipore). 30 µg of protein from the whole-cell lysate of each sample were loaded as input. The membranes were blocked with 5% BSA in wash buffer (Tris-buffered saline with 0.1% Tween 20) for 1 h at room temperature and probed with primary antibody overnight at a dilution recommended by the suppliers. Membranes were washed three times with wash buffer and then incubated with alkaline phosphatase-conjugated secondary antibody and detected by hydrolysis of BCIP chromogenic substrate according to the manufacturer's instruction.

Isolation of the nuclear fraction
To prepare subcellular fractions, the cells were lysed by a 10 min hypotonic treatment on ice in buffer A [10 mm HEPES (pH 7.9), 10 mm KCl, 1.5 mm
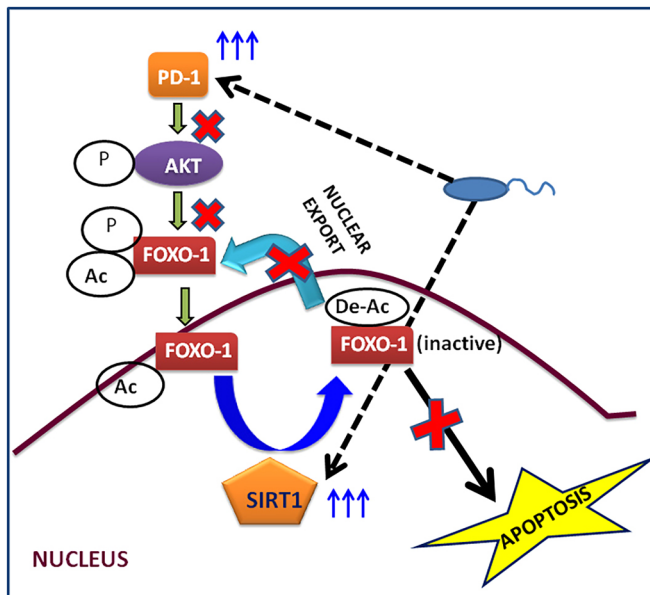
Fig. 8. Crosstalk between PD-1 and the SIRT1/FOXO-1 signaling axis during evasion of macrophage apoptosis and parasite survival. The late phase of *L. donovani* infection induces PD-1 signaling, which leads to the inactivation of AKT followed by the nuclear sequestration of FOXO-1. Concomitant with PD-1 upregulation, the late phase of *Leishmania* infection also induces SIRT1 expression, which deacetylates nuclear FOXO-1 and thereby inactivates it. SIRT1-mediated deacetylation of FOXO-1 subsequently prevents apoptosis.

MgCl$_2$, 0.5 mm DTT, 0.5 mM phenylmethylsulfonyl fluoride, 10 µg of leupeptin per ml, 10 µg of pepstatin per ml, 0.01 U of aprotinin per ml] followed by homogenization using a narrow gauge syringe. The extract was then centrifuged at 4°C for 10 min at 10,000 *g*. The supernatant was collected as the cytosolic extract. The pellet was washed once with ice-cold buffer A and resuspended in two volumes of buffer B [20 mm HEPES pH 7.9, 0.42 m NaCl, 1.5 mm MgCl$_2$, 0.2 mm EDTA, 0.5 mm dithiothreitol (DTT), 0.5mm phenylmethylsulfonyl fluoride, 10 µg of leupeptin per ml, 10 µg of pepstatin per ml, 0.01 U of aprotinin per ml and 25% glycerol]. After the concentration of NaCl was adjusted to 0.38 M, the suspension was kept at −70°C for 10 min, thawed slowly on ice and then incubated for 10 min in ice with intermittent tapping. After a 15 min centrifugation at 10,000 *g* at 4°C, the supernatant solution, representing the soluble nuclear fraction, was removed.

siRNA transfection
RAW 264.7 cells (2×10^6) were transfected with 1 µg of SIRT1 siRNA according to the manufacturer's instructions (Santa Cruz Biotechnology). Scrambled siRNA was used as control. After silencing, cells were infected with *L. donovani* promastigotes as described above.

Caspase 3 activity assay
Cells were washed twice with ice-cold PBS, resuspended in 50 µl of ice-cold lysis buffer [1 mM DL-dithiothreitol, 0.03% Nonidet P-40 (v/v), in 50 mM Tris-HCl pH 7.5], kept on ice for 30 min and finally centrifuged at 14,000 *g* for 15 min at 4°C. 10 µg of total protein was incubated with the caspase 3 substrate (Ac-DEVD-pNA) for 1 h at 37°C. The absorption was measured with a spectrophotometer at 405 nm.

NBT reduction assay
Total ROS or superoxide production was measured in isolated macrophages by measuring their ability to reduce NBT. Macrophages were treated with NBT (100 µl, 20 mg/ml; Sigma-Aldrich) dissolved in PBS incubated for 60–90 min at 37°C. Supernatants were discarded and cells were washed several times with 70% methanol and allowed to dry. Formed formazan was

solubilized by adding 100 µl/well KOH (2 M), followed by 100 µl/well DMSO. Absorbance was measured at 630 nm.

Measurement of NO
Nitrite accumulation in the culture supernatant fluids of macrophages and splenocytes was measured by the Griess reagent assay as previously described (Kar et al., 2010). For *in vivo* experiments, splenocytes were stimulated with 5 µg/ml soluble leishmanial antigen for 48 h prior to the Griess reagent assay.

Cytokine analysis by ELISA
The level of various cytokines in the culture supernatants of macrophages were measured by using a sandwich ELISA kit (Quantikine M, R&D Systems) as per the instructions of the manufacturer.

Fluorescence microscopy
Macrophages (10^5) were plated onto 18 mm^2 coverslips and cultured overnight. The cells were treated as mentioned and infected with *L. donovani* promastigotes, washed twice in PBS, and fixed with 4% formaldehyde for 30 min at room temperature. The cells were permeabilized with 0.1% Triton X and incubated with blocking solution followed by primary antibody for 1 h at 4°C. After washing, coverslips were incubated with FITC-conjugated secondary antibody for 1 h at room temperature. The cells were stained with DAPI (1 µg/ml) in PBS plus 10 µg/ml RNase A to label the nucleus, mounted on slides and visualized under a Olympus IX81 microscope equipped with a FV1000 confocal system using a 100× or 60× oil immersion Plan Apo (NA 1.45) objective. The images thus captured were analyzed by Olympus Fluoview (version 3.1a; Tokyo, Japan) using the colocalization program and assembled with Adobe Photoshop software.

Densitometric analysis
Densitometric analyses for all experiments were carried out using QUANTITY ONE software (Bio-Rad, Hercules, CA). Band intensities were quantitated densitometrically, and the values were normalized to that in the endogenous control and expressed in arbitrary units. The ratios of optical density of particular bands to that of the endogenous control are indicated as bar graphs adjacent to figures.

Statistical analysis
Data shown are representative of at least three independent experiments unless otherwise stated as *n* values given in the legend. Macrophage cultures were set in triplicates and the results are expressed as the mean±s.d. A Student's *t*-test was employed to assess the statistical significances of differences among pair of data sets with a *P*<0.05 considered to be significant.

Competing interests
The authors declare no competing or financial interests.

Author contributions
Conceptualization: S.R., A.U., P.K.D.; Methodology: S.R., S.S., A.U., P.K.D.; Validation: S.R., A.U., P.K.D.; Formal analysis: S.R., A.U., P.K.D.; Investigation: S.R., A.U., P.K.D. Data curation: S.S., P.G.; Writing - original draft: S.R., A.U., P.K.D.; Writing - review & editing: S.R., A.U., P.K.D.; Visualization: S.R., A.U., P.K.D.; Supervision: P.K.D.; Project administration: P.K.D.; Funding acquisition: P.K.D.

Supplementary information

Supplementary information available online at
http://jcs.biologists.org/lookup/doi/10.1242/jcs.226274.supplemental

References

Akarid, K., Arnoult, D., Micic-Polianski, J., Sif, J., Estaquier, J. and Ameisen, J. C. (2004). Leishmania major-mediated prevention of programmed cell death induction in infected macrophages is associated with the repression of mitochondrial release of cytochrome c. *J. Leukoc. Biol.* 76, 95-103. doi:10.1189/jlb.1001877

Alcendor, R. R., Gao, S., Zhai, P., Zablocki, D., Holle, E., Yu, X., Tian, B., Wagner, T., Vatner, S. F. and Sadoshima, J. (2007). Sirt1 regulates aging and resistance to oxidative stress in the heart. *Circ. Res.* 100, 1512-1521. doi:10.1161/01.RES.0000267723.65696.4a

Brunet, A., Bonni, A., Zigmond, M. J., Lin, M. Z., Juo, P., Hu, L. S., Anderson, M. J., Arden, K. C., Blenis, J. and Greenberg, M. E. (1999). Akt promotes cell survival by phosphorylating and inhibiting a Forkhead transcription factor. *Cell* 96, 857-868. doi:10.1016/S0092-8674(00)80595-4

Cantó, C. and Auwerx, J. (2009). Caloric restriction, SIRT1 and longevity. *Trends Endocrinol. Metab.* 20, 325-331. doi:10.1016/j.tem.2009.03.008

Chen, C.-J., Yu, W., Fu, Y.-C., Wang, X., Li, J.-L. and Wang, W. (2009). Resveratrol protects cardiomyocytes from hypoxia-induced apoptosis through the SIRT1-FoxO1 pathway. *Biochem. Biophys. Res. Commun.* 378, 389-393. doi:10.1016/j.bbrc.2008.11.110

Chen, W., Wang, J., Jia, L., Liu, J. and Tian, Y. (2016). Attenuation of the programmed cell death-1 pathway increases the M1 polarization of macrophages induced by zymosan. *Cell Death Dis.* 7, e2115. doi:10.1038/cddis.2016.33

Dey, R., Majumder, N., Bhattacharjee, S., Majumdar, S. B., Banerjee, R., Ganguly, S., Das, P. and Majumdar, S. (2007). Leishmania donovani-induced ceramide as the key mediator of Akt dephosphorylation in murine macrophages: role of protein kinase Czeta and phosphatase. *Infect. Immun.* 75, 2136-2142. doi:10.1128/IAI.01589-06

Ghosh, K., Sharma, G., Saha, A., Kar, S., Das, P. K. and Ukil, A. (2013). Successful therapy of visceral leishmaniasis with curdlan involves T-helper 17 cytokines. *J. Infect. Dis.* 207, 1016-1025. doi:10.1093/infdis/jis771

Ishida, Y., Agata, Y., Shibahara, K. and Honjo, T. (1992). Induced expression of PD-1, a novel member of the immunoglobulin gene superfamily, upon programmed cell death. *EMBO J.* 11, 3887-3895. doi:10.1002/j.1460-2075.1992.tb05481.x

Joshi, T., Rodriguez, S., Perovic, V., Cockburn, I. A. and Stäger, S. (2009). B7-H1 blockade increases survival of dysfunctional CD8(+) T cells and confers protection against Leishmania donovani infections. *PLoS Pathog.* 5, e1000431. doi:10.1371/journal.ppat.1000431

Kar, S., Ukil, A., Sharma, G. and Das, P. K. (2010). MAPK-directed phosphatases preferentially regulate pro- and anti-inflammatory cytokines in experimental visceral leishmaniasis: involvement of distinct protein kinase C isoforms. *J. Leukoc. Biol.* 88, 9-20. doi:10.1189/jlb.0909644

Keir, M. E., Butte, M. J., Freeman, G. J. and Sharpe, A. H. (2008). PD-1 and its ligands in tolerance and immunity. *Annu. Rev. Immunol.* 26, 677-704. doi:10.1146/annurev.immunol.26.021607.090331

Ma, C. J., Ni, L., Zhang, Y., Zhang, C. L., Wu, X. Y., Atia, A. N., Thayer, P., Moorman, J. P. and Yao, Z. Q. (2011). PD-1 negatively regulates interleukin-12 expression by limiting STAT-1 phosphorylation in monocytes/macrophages during chronic hepatitis C virus infection. *Immunology* 132, 421-431. doi:10.1111/j.1365-2567.2010.03382.x

Michan, S. and Sinclair, D. (2007). Sirtuins in mammals: insights into their biological function. *Biochem. J.* 404, 1-13. doi:10.1042/BJ20070140

Mühlbauer, M., Fleck, M., Schütz, C., Weiss, T., Froh, M., Blank, C., Schölmerich, J. and Hellerbrand, C. (2006). PD-L1 is induced in hepatocytes by viral infection and by interferon-alpha and -gamma and mediates T cell apoptosis. *J. Hepatol.* 45, 520-528. doi:10.1016/j.jhep.2006.05.007

Roy, S., Gupta, P., Palit, S., Basu, M., Ukil, A. and Das, P. K. (2017). The role of PD-1 in regulation of macrophage apoptosis and its subversion by Leishmania donovani. *Clin. Transl. Immunol.* 6, e137. doi:10.1038/cti.2017.12

Ruhland, A., Leal, N. and Kima, P. E. (2007). Leishmania promastigotes activate PI3K/Akt signalling to confer host cell resistance to apoptosis. *Cell. Microbiol.* 9, 84-96. doi:10.1111/j.1462-5822.2006.00769.x

Salminen, A., Kauppinen, A., Suuronen, T. and Kaarniranta, K. (2008). SIRT1 longevity factor suppresses NF-kappaB -driven immune responses: regulation of aging via NF-kappaB acetylation? *BioEssays* 30, 939-942. doi:10.1002/bies.20799

Shi, F., Shi, M., Zeng, Z., Qi, R.-Z., Liu, Z.-W., Zhang, J.-Y., Yang, Y.-P., Tien, P. and Wang, F.-S. (2011). PD-1 and PD-L1 upregulation promotes CD8(+) T-cell apoptosis and postoperative recurrence in hepatocellular carcinoma patients. *Int. J. Cancer* 128, 887-896. doi:10.1002/ijc.25397

Srivastav, S., Basu Ball, W., Gupta, P., Giri, J., Ukil, A. and Das, P. K. (2014). Leishmania donovani prevents oxidative burst-mediated apoptosis of host macrophages through selective induction of suppressors of cytokine signaling (SOCS) proteins. *J. Biol. Chem.* 289, 1092-1105. doi:10.1074/jbc.M113.496323

Tzivion, G., Dobson, M. and Ramakrishnan, G. (2011). FoxO transcription factors; Regulation by AKT and 14-3-3 proteins. *Biochim. Biophys. Acta* 1813, 1938-1945. doi:10.1016/j.bbamcr.2011.06.002

Wang, W., Yan, C., Zhang, J., Lin, R., Lin, Q., Yang, L., Ren, F., Ji, M. and Li, Y. (2013). SIRT1 inhibits TNF-alpha-induced apoptosis of vascular adventitial fibroblasts partly through the deacetylation of FoxO1. *Apoptosis* 18, 689-701. doi:10.1007/s10495-013-0833-7

Wang, Y., Zhou, Y. and Graves, D. T. (2014). FOXO transcription factors: their clinical significance and regulation. *Biomed. Res. Int.* 2014, 925350. doi:10.1155/2014/925350

Winnik, S., Stein, S. and Matter, C. M. (2012). SIRT1 - an anti-inflammatory pathway at the crossroads between metabolic disease and atherosclerosis. *Curr. Vasc. Pharmacol.* 10, 693-696. doi:10.2174/157016112803520756

Yang, Y., Zhao, Y., Liao, W., Yang, J., Wu, L., Zheng, Z., Yu, Y., Zhou, W., Li, L., Feng, J. et al. (2009). Acetylation of FoxO1 activates Bim expression to induce apoptosis in response to histone deacetylase inhibitor depsipeptide treatment. *Neoplasia* 11, 313-324. doi:10.1593/neo.81358

Yang, H., Zhang, W., Pan, H., Feldser, H. G., Lainez, E., Miller, C., Leung, S., Zhong, Z., Zhao, H., Sweitzer, S. et al. (2012). SIRT1 activators suppress inflammatory responses through promotion of p65 deacetylation and inhibition of NF-kappaB activity. *PLoS ONE* 7, e46364. doi:10.1371/journal.pone.0046364

Yoshizaki, T., Milne, J. C., Imamura, T., Schenk, S., Sonoda, N., Babendure, J. L., Lu, J.-C., Smith, J. J., Jirousek, M. R. and Olefsky, J. M. (2009). SIRT1 exerts anti-inflammatory effects and improves insulin sensitivity in adipocytes. *Mol. Cell. Biol.* 29, 1363-1374. doi:10.1128/MCB.00705-08

Zhang, X., Tang, N., Hadden, T. J. and Rishi, A. K. (2011). Akt, FoxO and regulation of apoptosis. *Biochim. Biophys. Acta* 1813, 1978-1986. doi:10.1016/j.bbamcr.2011.03.010